Inclusive Δ^{++} production in pp, K^+p, π^+p, and π^-p interactions at 147 GeV/c

D. Brick, A. M. Shapiro, and M. Widgoff
Brown University, Providence, Rhode Island 02912

R. E. Ansorge, J. R. Carter, W. W. Neale, J. G. Rushbrooke, D. R. Ward, and B. M. Whyman
University of Cambridge, Cambridge, England

R. A. Burnstein and H. A. Rubin
Illinois Institute of Technology, Chicago, Illinois 60616

J. W. Cooper, R. L. Plumer,* R. D. Sard, and J. O. Tortora†
University of Illinois, Urbana, Illinois 61801

E. D. Alyea
Indiana University, Bloomington, Indiana 47401

L. Bachman,‡ C.-Y. Chien, and A. Pevsner
Johns Hopkins University, Baltimore, Maryland 21218

J. E. Brau,§ E. S. Hafen, D. Hochman,‖ R. I. Hulsizer, V. Kistiakowsky, A. Levy,¶ P. Lutz,** A. Napier,††
I. A. Pless, J. P. Silverman,‡‡ P. C. Trepagnier, and R. K. Yamamoto
Laboratory for Nuclear Science and Department of Physics, Massachusetts Institute of Technology, Cambridge, Massachusetts 02139

F. Grard, J. Hanton, V. Henri, P. Herquet, J. M. Lesceux, and R. Windmolders
Université de l'Etat, Mons, Belgium

F. Crijns, H. deBock, W. Kittel, W. Metzger, C. Pols, M. Schouten, and R. Van de Walle
University of Nijmegen, Nijmegen, The Netherlands

H. O. Cohn
Oak Ridge National Laboratory, Oak Ridge, Tennessee 37830

G. Bressi, E. Calligarich, C. Castoldi, G. Cecchet, R. Dolfini, G. Liguori, and S. Ratti
University of Pavia and INFN, Pavia, Italy

P. F. Jacques, M. Kalelkar, R. J. Plano, P. Stamer, and T. L. Watts
Rutgers University, New Brunswick, New Jersey 08903

E. B. Brucker, E. L. Koller, and S. Taylor
Stevens Institute of Technology, Hoboken, New Jersey 08903

L. Berny, S. Dado, J. Goldberg, and S. Toaff
Technion, Haifa, Israel

G. Alexander, O. Benary, S. Dagan, J. Grunhaus, D. Lissauer, and Y. Oren
Tel-Aviv University, Ramat-Aviv, Israel

W. M. Bugg, G. T. Condo, T. Handler, and E. L. Hart
University of Tennessee, Knoxville, Tennessee 37916

Y. Eisenberg, U. Karshon, E. E. Ronat, A. Shapira, R. Yaari, and G. Yekutieli
Weizmann Institute of Science, Rehovot, Israel

D. A. Ljung,§§ T. W. Ludlam,‖‖ and H. D. Taft
Yale University, New Haven, Connecticut 06520

(Received 5 September 1979)

We have studied inclusive Δ^{++} production at 147 GeV/c in pp, K^+p, π^+p, and π^-p interactions. All four reactions were detected with the same apparatus and analyzed in the same way. The energy dependence of the Δ^{++} cross section was found to be $Ap^{-1}+B$ for pp, K^+p, and π^+p interactions and constant for π^-p interactions. The shape of the inclusive Δ^{++} distributions does not depend on the beam, while the magnitudes are proportional to the total cross sections. We have obtained the effective trajectory at the p-Δ^{++} vertex from a triple-Regge analysis and found that all results are consistent with predictions of a triple-Regge diagram where a Pomeron is exchanged at the beam vertex and a π at the target vertex.

I. INTRODUCTION

This is a report on a comparative study of Δ^{++} inclusive production at 147 GeV/c in π^+p, K^+p, pp, and π^-p interactions. Systematic differences among the four interactions have been minimized by the fact that all these interactions have been measured at the same energy with the same apparatus and have been analyzed using the same procedure. In this paper we present new results for the reaction

$$pp \to \Delta^{++} + X^0 \tag{1}$$

and for the reactions

$$K^+p \to \Delta^{++} + X^0 \tag{2}$$

and

$$\pi^+p \to \Delta^{++} + X^0 \tag{3}$$

at the highest energy to date. The results of the reaction

$$\pi^-p \to \Delta^{++} + X^{--} \tag{4}$$

have been previously published elsewhere.[1]

We find that the shapes of the inclusive distributions of Δ^{++} production in reactions (1)–(4) are independent of the identity of the incoming beam particle. The relative magnitudes of the inclusive cross sections for these reactions are in good agreement with the predictions of a triple-Regge model. We have used this model to extract the effective trajectory at the $p\Delta^{++}$ vertex.

The experimental details are presented in Sec. II. The cross sections for reactions (1)–(4) are given in Sec. III, where we also discuss their energy dependence. Some inclusive distributions are shown in Sec. IV. Section V contains the results of a triple-Regge analysis of the data. The results are summarized and conclusions are given in Sec. VI.

II. EXPERIMENTAL DETAILS

The data used in the present study come from two exposures in the Fermilab 30-inch hybrid spectrometer; one with a tagged negative beam, mainly π^-, and one with a tagged positive beam composed of π^+, K^+, and p. Beam particle identification was made by a threshold and differential Čerenkov counter. In both exposures, the beam momentum was 147 GeV/c. The results of the 105 000-picture π^-p exposure have already been published.[1,2] The 400 000-picture positive-beam exposure consisted of two parts: one in which the beam content was mainly π^+ and p with a very small number of K^+'s and another with the ratio of $\pi^+/K^+/p$ of 6/1/3. A small prototype of a lead-glass forward-γ detector was added for the second part of the positive exposure. Details of the experimental arrangement and of the data reduction have already been published.[2]

The present study is based on 6974 π^-p events, 11 513 pp events, 12 561 π^+p events, and 1701 K^+p events. All of the events were analyzed in exactly the same manner. All negative outgoing particles and positive particles with laboratory momentum greater than 1.4 GeV/c were assumed to be pions. Positive particles with laboratory momentum less than 1.4 GeV/c were identified as π^+ or p by ionization.

The correct identification of protons is necessary for the study of reactions (1)–(4). Since this identification is limited to positively charged particles with laboratory momenta ≤ 1.4 GeV/c, one cannot study inclusive Δ^{++} production using identified protons over the whole $t_{p\Delta}$ range, where $t_{p\Delta}$ is the square of the four-momentum transfer between the target proton and the Δ. One can, as the authors of Ref. 3 among others have done, completely disregard ionization information and assign multiple mass hypotheses to each positive track, entering each hypothesis in the invariant-mass distribution. The t dependence of the false combinations at 16 GeV/c was checked and no significant structure was found in the Δ mass region.[3] For our present study, we have restricted ourselves only to identified proton events. To avoid biasing the angular distributions, we have further restricted the data sample to $|t_{p\Delta}| \leq 1$ $(\text{GeV}/c)^2$. This limits, of course, our study of reaction (1) to Δ^{++}'s produced in the backward center-of-mass hemisphere. The number of events in various topologies have been corrected for scanning and processing losses by normalization to the topological cross sections presented in Ref. 2. Further details of the data handling and the various corrections, most of which are topology dependent, can be found in Ref. 1.

III. Δ^{++} CROSS SECTION

Figure 1 shows the $p\pi^+$ mass distribution of all the combinations having a momentum transfer squared of $|t_{p,p\pi^+}| \leq 1$ $(\text{GeV}/c)^2$. The mass distributions resulting from the reaction $pp \to (p\pi^+)$ + anything, $K^+p \to (p\pi^+)$ + anything, $\pi^+p \to (p\pi^+)$ + anything, and $\pi^-p \to (p\pi^+)$ + anything are displayed in Figs. 1(a), 1(b), 1(c), and 1(d), respectively. All four reactions show clear peaks in the vicinity of the Δ^{++} mass.

Several techniques for estimating the cross section for Δ^{++} production in reactions (1)–(4) have been used in various experiments. The cross section has sometimes been estimated by a simple

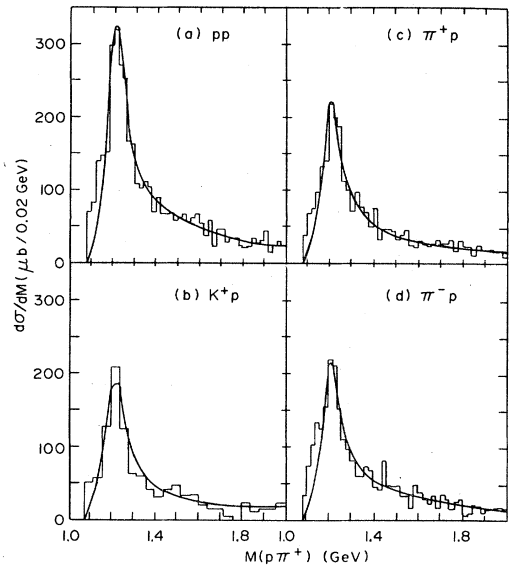

FIG. 1. Effective mass of $p\pi^+$ combinations for those combinations which satisfied the condition $|t_{p,p\pi^+}| \leq 1$ (GeV/c)^2 for the interactions (a) pp, (b) K^+p, (c) π^+p, and (d) π^-p, each at 147 GeV/c incident momentum. The curves shown are the results of the fits described in the text.

mass cut. The background has sometimes been described by a hand-drawn curve,[4] sometimes by fitting a polynomial expansion in the effective mass M of the $p\pi^+$ combination[1] or in $(M - M_{th})$,[5,6] where $M_{th} = m_p + m_\pi$, and sometimes by fitting an exponential in M to the data. Three forms used for the exponential background are e^{-aM},[3,7] $(M^2 - M_{th}^2)^b e^{-aM}$,[8] and $(M - M_{th})^b e^{-aM-cM^2}$,[9] where a, b, and c are fitted parameters.

There are also variations in the Breit-Wigner function used to describe the data. One form used is[10]

$$F_{BW} = \frac{M}{q} \frac{\Gamma(M)}{(M^2 - M_0^2)^2 + M_0^2 \Gamma^2(M)}, \tag{5}$$

where

$$\Gamma = \Gamma_0 \left(\frac{q}{q_0}\right)^3 \frac{\rho(M)}{\rho(M_0)}.$$

The quantities M_0 and Γ_0 are the mass and width of the Δ^{++}, respectively, and q is the momentum of one of the decay products in the Δ^{++} rest frame. The forms used for $\rho(M)$ are $\rho(M) = (m_\pi^2 + q^2)^{-1}$,[3] $\rho(M) = (2.2 m_\pi^2 + q^2)^{-1}$,[1] and $\rho(M) = [(M + m_p)^2 - M_\pi^2]/M^2$.[9] Another form for the Breit-Wigner function is

$$F_{BW} = \frac{M_0 \Gamma}{(M^2 - M_0^2)^2 + M^2 \Gamma^2}, \tag{6}$$

where $\Gamma = \Gamma_0 (q/q_0)^3$.[6]

The cross section obtained for Δ^{++} production has been found to depend on the method used to obtain it.[6] Thus, any comparative study of the Δ^{++} production must use a consistent method of obtaining the Δ^{++} cross section. In the present paper we study both the energy dependence and the beam dependence of the Δ^{++} production. The method used to obtain the Δ^{++} cross section for the study of the energy dependence of each of the reactions (1)–(4) will be that used for the same particular reaction at other energies. For our study of the beam dependence of the Δ^{++} production, we will use the method discussed later in this section for all four reactions.

Reaction (1) has been studied at beam momenta up to 405 GeV/c. The $p\pi^+$ mass distributions in the energy range 12 to 405 GeV/c have been fitted[7] to the form

$$\frac{d\sigma}{dM} = A e^{-bM} (q + C F_{BW}), \tag{7}$$

where M is the mass of the $p\pi^+$ combination, q the momentum of one of the decay products at this mass, and F_{BW} represents a p-wave Breit-Wigner function. We have fitted this form to our mass distribution of Fig. 1(a) over the same mass range as used in Ref. 7 (1.08–1.52 GeV). Figure 2(a) shows our results at 147 GeV/c together with the results of Ref. 7. The cross section for reaction (1) decreases with P_{lab}, then levels off near 70 GeV/c to a constant value of about 1.3 mb with a possible rise at higher energies.

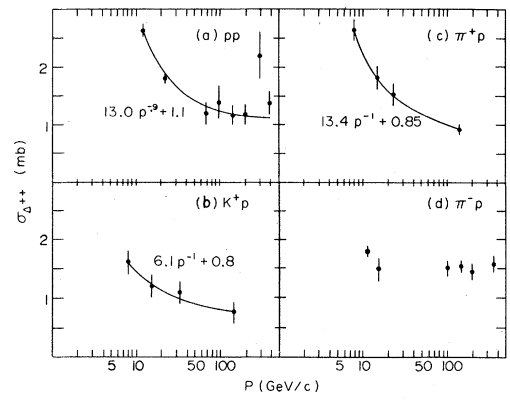

FIG. 2. Variation of inclusive Δ^{++} cross section as a function of laboratory momentum for (a) pp interactions at 147 GeV/c with $|t| < 1$ (GeV/c)^2 (in the backward hemisphere), along with data compiled in Ref. 7; (b) K^+p interactions at 147 GeV/c with $|t| < 1$ (GeV/c)^2, along with cross sections based on data in Ref. 9; (c) π^+p interactions at 147 GeV/c with $|t| < 0.6$ (GeV/c)^2, along with cross sections based on data in Ref. 11; (d) π^-p interactions at 147 GeV/c with $|t| < 1$ (GeV/c)^2, along with data from Refs. 6 and 12.

Reaction (2) has been studied at beam momenta up to 32 GeV/c.[9] Our experiment extends the highest energy measurement of reaction (2) to 147 GeV/c, permitting a good determination of the energy dependence of the Δ^{++} cross section. Reaction (2) has been fitted[9] to the form

$$\frac{d\sigma}{dM} = \alpha_2 (M - M_{\text{th}})^{\alpha_3} e^{-\alpha_4 M - \alpha_5 M^2} (1 + \alpha_1 F_{\text{BW}}), \quad (8)$$

where F_{BW} has the form (5) with $\rho(M) = [(M + m_p)^2 - m_\pi^2]/M^2$, and the α_i are fitted parameters. This fit was performed at 32 GeV/c for different t intervals, using the method of Ref. 3, and the resulting t distribution was presented up to 3 (GeV/c)^2.[9] We have used the t distribution of Ref. 9 to deduce their integrated Δ^{++} cross section for $|t| < 1$ (GeV/c)^2. If we assume that the Δ^{++} has the same t dependence at 8.25, 16, and 32 GeV/c, we can obtain an estimate of the Δ^{++} cross section at these energies for $|t| < 1$ (GeV/c)^2. We have fitted Eq. (8) to our data for reaction (2) and present our result at 147 GeV/c in Fig. 2(b), together with these estimated cross sections at 8.25, 16, and 32 GeV/c. The energy behavior of reaction (2) is similar to that of reaction (1). Although the cross section can be seen to decrease with energy, more data points are needed at intermediate energies and at higher energies to see whether it has reached a constant value at our energy.

The cross section for reaction (3) has been given at various energies but these measurements cannot be directly compared because they were obtained using different techniques. Distributions of $d\sigma/(dt\,dM)$ for $M(p\pi^+) = 1.12$–1.34 GeV and $|t| < 0.6$ (GeV/c)^2 have been published at 8, 16, and 23 GeV/c.[11] The cross section we obtain at 147 GeV/c for $p\pi^+$ combinations wtih $M(p\pi^+) = 1.12$–1.34 GeV and $|t| < 0.6$ (GeV/c)^2 is shown in Fig. 2(c), together with the integrated values from the lower energies.[11] The cross section decreases toward a possibly constant value, as in the other two reactions.

Reaction (4), which has been measured at incident momenta up to 360 GeV/c,[6] exhibits a different energy behavior. In fact, the cross section is nearly constant from 10 to 360 GeV/c. We have fitted our $p\pi^+$ mass distribution from reaction (4) to the form used in Ref. 6,

$$\frac{d\sigma}{dM} = aF_{\text{BW}} + \sum_{i=1}^{2} b_i (M - M_{\text{th}})^i, \quad (9)$$

where F_{BW} has the form (6). The cross section we obtained for reaction (4) at 147 GeV/c using this technique is shown in Fig. 2(d), along with the values obtained in Ref. 6 and at other energies.[12] As can be seen, the cross section is almost constant throughout the energy range 10–360 GeV/c.

Due to the fact that the cross sections for reactions (1)–(4) were obtained using different techniques, one cannot compare the absolute cross-section values. Nevertheless, one can make qualitative comparisons of the energy dependence of the four reactions. There is a clear difference between the Δ^{++} cross sections obtained with a p, K^+, or π^+ beam and that obtained with a π^- beam; in reactions (1), (2), and (3), we have observed a decrease of the cross section towards an almost constant, or even rising, value with energy. In contrast, reaction (4) has an almost constant cross section. This different behavior is not surprising if one considers the recoiling system; in reaction (4) the recoiling system is exotic, does not contain resonances, and, thus, one expects Pomeron dominance at the vertex of the recoiling system. Such behavior was also found for the reaction $K^-p \to \Delta^{++}X^{--}$, when the cross section also seems to remain constant to the highest available measurement at 32 GeV/c.[13]

Reactions (1)–(3), on the other hand, have a neutral recoiling system and, thus, can include two-body final states like $\Delta^{++}\rho^0$, $\Delta^{++}\omega$, $\Delta^{++}f^0$, etc. These processes are known to give sizable contributions to the cross section at lower energies—contributions which are expected to decrease with energy. Thus, whereas Pomeron exchange dominates already at relatively low energies in reaction (4), here there are two contributions, Reggeon exchange and Pomeron exchange. Reggeon exchange is expected to have a $p^{-\alpha}$ decrease with laboratory momentum p, where α is a fitted parameter; the Pomeron-exchange contribution is constant with energy. We have fitted the cross-section values of reactions (1)–(3) to the form

$$\sigma = Ap^{-\alpha} + B, \quad (10)$$

where σ is the cross section in mb, and A, α, and B are fitted parameters. The results of our fits, shown as the solid lines in Fig. 2, are all consistent with a p^{-1} behavior. The best fit values of the parameter α are 0.9 ± 0.1, 1.0 ± 0.2, and 1.0 ± 0.2 for reactions (1), (2), and (3), respectively. Reaction (4) has no energy dependence, as expected.[14]

We would like to compare the details of the reactions (1)–(4) with each other in order to study the dependence of inclusive Δ^{++} production on the quantum numbers of the initial state. As previously stated, we cannot use the values given in Fig. 2 for this purpose because they were evaluated by a different method for each beam. Therefore, we have fitted the $p\pi^+$ mass distributions of all four reactions to the same expression

$$\frac{d\sigma}{dM} = \alpha F_{BW} + \sum_{i=1}^{3} b_i (M - M_{th})^i , \qquad (11)$$

where

$$F_{BW} = \frac{M\Gamma}{q[(M_0^2 - M^2)^2 + M_0^2\Gamma^2]} , \quad \Gamma = \Gamma_0 \left(\frac{q}{q_0}\right)^3 \frac{\rho(M)}{\rho(M_0)} .$$

$\rho(M) = (2.2m_\pi^2 + q^2)^{-1}$, $M_0 = 1.228$ GeV, and $\Gamma_0 = 0.123$ GeV. The fit was performed over the mass range $M(p\pi^+) < 2$ GeV and $|t| < 1$ (GeV/c)^2. The curve corresponding to the best fit of expression (11) to the data can be seen in Fig. 1. The mass parametrization of Eq. (11) is one of several that give an adequate representation of the $p\pi^+$ mass distribution . A fourth term in the polynomial improves the χ^2 contribution at low masses but does not change the cross section; including the third term does alter the cross section. The important point is that the same technique be used for all four reactions. The cross sections obtained by fitting Eq. (11) to the mass distributions are given in Table I for all four reactions. The cross sections displayed in Table I do not correspond to any of these displayed in Fig. 2, since the technique used here is different from those used to obtain Fig. 2. The Δ^{++} cross section for pp reactions is in the backward hemisphere only. We have also performed a fit to the mass distribution for each topology, results of which are also given in Table I. The Δ^{++} cross section for a π^+ beam is about equal to that for a π^- beam; the pp cross section is about 40% higher than the π^-p and the K^+p is about 20% smaller than the π^-p. Let us define R_a as the ratio of Δ^{++} cross sections to the total cross section for an incident particle a,

$$R_a \equiv \frac{\sigma(ap \to \Delta^{++}X)}{\sigma_T(ap)} . \qquad (12)$$

The values of R_a are listed in Table I for the four incoming beam particles. These values are equal to each other within uncertainties.

In Table I we also give the topological and total cross sections for the mass region $1.12 < M(p\pi)^+ < 1.32$ GeV and for $|t| < 1$ (GeV/c)^2. This mass cut gives results which are very close to those obtained by fitting the mass distributions in Fig. 1. A further comparison of the Δ^{++} cross section for the four reactions will be given in Sec. V.

TABLE I. Fitted Δ^{++} cross sections (in mb) for $|t| < 1$ (GeV/c)^2 and cross sections for events with $1.12 < M(p\pi^+) < 1.32$ GeV and $|t| < 1$ (GeV/c)^2. R_a is the ratio of the Δ^{++} cross section to the total cross section in a given reaction.

	pp		K^+p		π^+p		π^-p	
Topology	Fit	Mass cut	Fit	Mass cut	Fit	Mass cut	Fit	Mass cut
4	0.56±0.06	0.55±0.04	0.36±0.09	0.27±0.05	0.36±0.03	0.30±0.02	0.36±0.04	0.29±0.03
6	0.63±0.07	0.59±0.04	0.31±0.11	0.33±0.06	0.42±0.04	0.40±0.03	0.29±0.04	0.31±0.03
8	0.41±0.06	0.43±0.04	0.29±0.10	0.32±0.06	0.31±0.04	0.29±0.02	0.26±0.04	0.33±0.03
10	0.22±0.04	0.23±0.03	0.07±0.07	0.15±0.04	0.16±0.03	0.17±0.02	0.20±0.04	0.24±0.02
12–16	0.16±0.04	0.22±0.03	0.07±0.05	0.09±0.03	0.16±0.03	0.18±0.02	0.16±0.04	0.23±0.02
all	2.03±0.12	2.01±0.08	1.15±0.18	1.16±0.10	1.43±0.07	1.33±0.05	1.36±0.09	1.38±0.07
R_a	0.053±0.003	0.052±0.002	0.059±0.009	0.060±0.005	0.062±0.003	0.057±0.002	0.056±0.004	0.057±0.003

IV. INCLUSIVE Δ^{++} DISTRIBUTIONS

In this section we present the inclusive differential cross section of the Δ^{++} in the variables $t' = |t - t_{min}|$, the square of the transverse momentum (p_T^2), Feynman x, and the rapidity in the center of mass (y). These distributions will be given for all four reactions (1)–(4). For reactions

(1), (3), and (4), the distributions were obtained in two ways: (a) The data were divided into appropriate regions of the inclusive variable, and the $p\pi^+$ mass distribution was fitted for the amount of Δ^{++} cross section in each region using the form (11); (b) the distribution was obtained for the mass interval $1.12 < M(p\pi^+) < 1.32$ GeV. As we have already shown in Table I for the total cross sections, and as can be seen in the inclusive distributions, both methods give very similar results. The number of events in our sample of reaction (2) is a factor of 5 smaller than the number of events in the other three reactions, so some distributions for reaction (2) were obtained only by the mass cut method.

A. t' distribution

The t' distribution can be used to show the peripheral nature of the mechanism responsible for Δ^{++} production. Figure 3 shows the t' distribution of Δ^{++} produced in reactions (1)–(4), as obtained by the two methods described above. A single exponential distribution was fitted to the mass cut data for all four distributions, using the data up to $t' = 0.4$ (GeV/c)^2. The resulting slope parameters are given in Table II. As can be seen, reactions (2), (3), and (4) have almost the same slope, while reaction (1) has a slightly steeper slope.

TABLE II. Fitted parameters for $d\sigma/dt' = Ae^{-bt'}$ and for $d\sigma/dp_T^2 = Ce^{-Bp_T^2}$.

	pp	K^+p	π^+p	π^-p
b [(GeV/c)$^{-2}$]	6.7±0.4	5.4±1.1	5.2±0.4	5.5±0.4
B [(GeV/c)$^{-2}$]	8.9±0.4	8.2±1.1	7.0±0.4	7.4±0.5

Similar slopes are obtained over the same t' interval at other energies. The steepness of the slope indicates that Δ^{++} production is peripheral and suggests that the production mechanism is consistent with a one-pion-exchange (OPE) model including absorption.[15] This will be further discussed in Sec. V.

B. p_T^2 distribution

The procedure used to obtain the transverse momentum distribution $d\sigma/dp_T^2$ for the Δ^{++} is similar to that used for the $d\sigma/dt'$ distribution described above. Figure 4 shows the $d\sigma/dp_T^2$ distribution for $p_T^2 \leq 0.4$ (GeV/c)^2 for all four reactions. We have fitted a single exponential to the mass cut distributions; the slopes are given in Table II. Reactions (2), (3), and (4) yield the same slopes within errors. The slope of reaction (1) is slightly higher than the others.

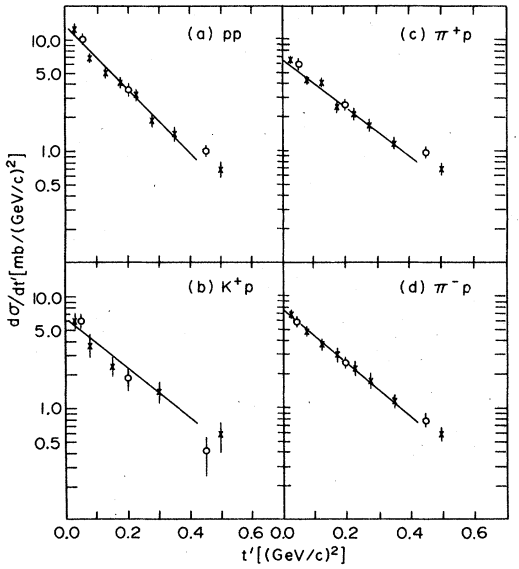

FIG. 3. Differential cross section $d\sigma/dt'$ as a function of t' for Δ^{++} production in (a) pp, (b) K^+p, (c) π^+p, and (d) π^-p interactions. The curves shown are the results of the fits described in the text. The crosses are vlaues obtained via mass cuts, the open circles are values obtained by fitting the $p\pi^+$ mass distribution for the t' ranges $0 \leq t' \leq 0.1$, $0.1 \leq t' \leq 0.3$, and $0.3 \leq t' \leq 0.6$ (GeV/c)^2.

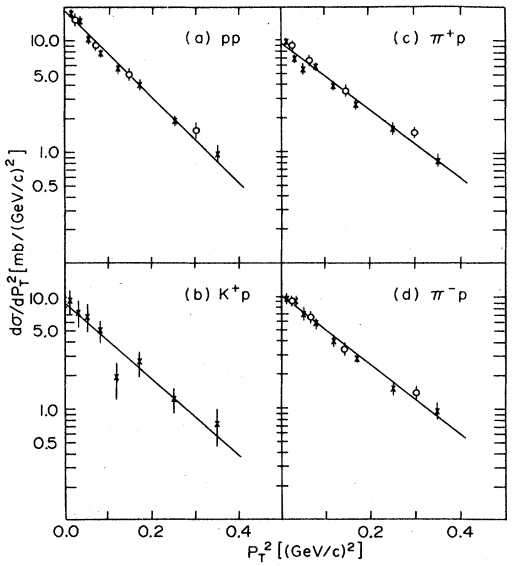

FIG. 4. Differential cross section $d\sigma/dp_T^2$ as a function of p_T^2 for Δ^{++} production in (a) pp, (b) K^+p, (c) π^+p, and (d) π^-p interactions. The curves shown are the results of the fits described in the text. The crosses are values obtained via mass cuts, the open circles are values obtained by fitting the $p\pi^+$ mass distributions for the p_T^2 ranges $0 \leq p_T^2 \leq 0.04$, $0.04 \leq p_T^2 \leq 0.1$, $0.1 \leq p_T^2 \leq 0.2$, and $0.2 \leq p_T^2 \leq 0.4$ (GeV/c)^2.

C. *x,y* distributions

Figures 5 and 6 show the Feynman x and rapidity y distributions of the Δ^{++}, respectively. For reactions (1), (3), and (4), we have obtained these distributions by both fitting the mass distributions in each x and y bin and by using a mass cut. The two methods give very similar results except for the region $x > -0.7$. In this region the overall $|t| < 1$ (GeV/c)^2 cut combined with the x cut severely limits the $p\pi^+$ mass distribution to low masses, below the central peak of the Δ^{++}. Thus, a mass cut for high x includes a larger fraction of low mass (below the Δ^{++}) combinations and thus overestimates the cross section in this region. For reaction (2) we used only the mass cut definition of Δ^{++} for these distributions. All four reactions have similar $d\sigma/dx$ and $d\sigma/dy$ distributions. The x distribution of the Δ^{++} peaks around $x = -0.85$ for all four reactions. This result is again in good agreement with the prediction of Gotsman[15] for an OPE model with absorption, which is that the x distribution should peak near -0.85 for $p_T^2 < 0.1$ (GeV/c)^2. The y distributions peak around $y = -2.4$ in all four reactions.

In summary, the Δ^{++} seems to have the same behavior in t', p_T^2, x, and y in all four reactions. This behavior is similar to that of Δ^{++} produced in K^-p (Ref. 16) and $\bar{p}p$ (Refs. 7, 8) reactions.

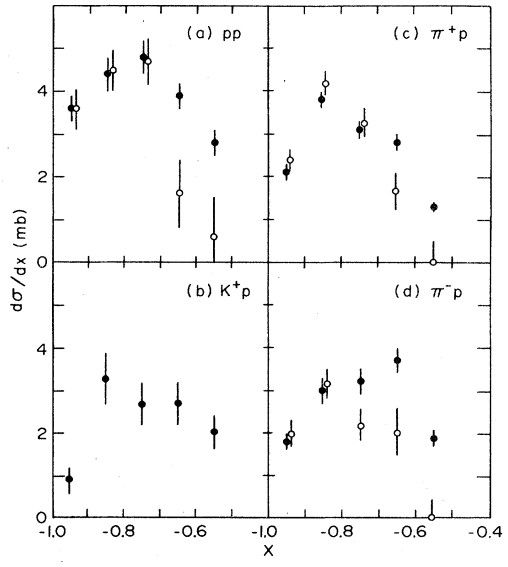

FIG. 5. Inclusive Δ^{++} production cross section as a function of x for (a) pp, (b) K^+p, (c) π^+p, and (d) π^-p interactions. The closed circles are the values obtained via mass cuts, the open circles are values obtained by fits to the $p\pi^+$ mass distributions.

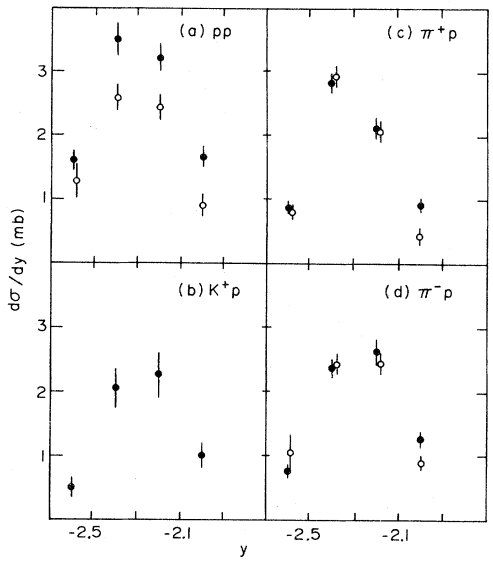

FIG. 6. Inclusive Δ^{++} production cross section as a function of y for (a) pp, (b) K^+p, (c) π^+p, and (d) π^-p interactions. The closed circles are the values obtained via mass cuts, the open circles are values obtained by fits to the $p\pi^+$ mass distributions.

V. TRIPLE-REGGE ANALYSIS

In this section we will study Δ^{++} production in the framework of the triple-Regge model. The schematic diagram for this process is shown in Fig. 7. We denote the trajectory coupled to the p-Δ^{++} vertex by E, the beam particle by a, and the exchange dominating the $aE \to aE$ scattering by M. Since the Δ^{++} cross section is constant or possibly rising at high energies for reactions (1), (3), (4), and possibly (2), we expect M to be the Pomeron. Pomeron exchange has been shown[5] to dominate already at 15 GeV/c in reaction (4). A further test of Pomeron dominance can be made by studying the ratio of Δ^{++} cross section to the total cross section, as defined in (12). If the Pomeron dom-

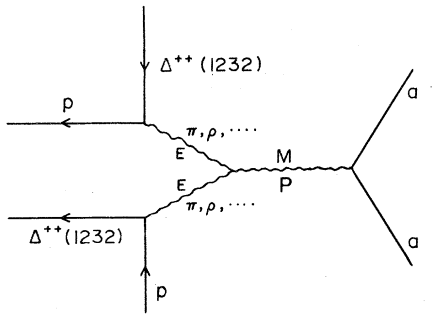

FIG. 7. Triple-Regge diagrammatic representation of the reaction $a\,p \to \Delta^{++}X$.

TABLE III. Δ^{++} density matrix elements for $t' < 0.2$ (GeV/c)^2. Our results and predictions for OPE with absorption (OPEA).

	pp	K^+p	π^+p	π^-p	OPEA
ρ_{33}	0.08±0.03	0.09±0.06	0.12±0.03	0.05±0.03	0.12
$\mathrm{Re}\rho_{31}$	−0.02±0.03	−0.08±0.07	0.02±0.03	−0.03±0.03	0.06
$\mathrm{Re}\rho_{3-1}$	0.02±0.03	0.01±0.08	−0.01±0.03	0.03±0.03	0.03

inates at the beam vertex in reactions (1)–(4), then Pomeron factorization would predict that the ratio between Δ^{++} cross sections for two different beam particles a and b should be equal to the ratio of the corresponding total cross sections σ_T

$$\frac{\sigma(bp \to \Delta^{++}X)}{\sigma(ap \to \Delta^{++}X)} = \frac{\sigma_T(bp)}{\sigma_T(ap)} \tag{13}$$

or, equivalently,

$$\frac{\sigma(ap \to \Delta^{++}X)}{\sigma_T(ap)} = \frac{\sigma(bp \to \Delta^{++}X)}{\sigma_T(bp)} .$$

These ratios are listed in Table I and are indeed equal to each other. The agreement for reaction (2) indicates that although Pomeron dominance could not be established from the energy dependence alone, it is in fact valid in that case as well. We will therefore make the assumption that M is the Pomeron in our triple-Regge analysis.

Next, we will consider the exchange E. The steep t' distribution and the shape of the x distributions were in agreement with predictions of an OPE model[15] suggesting that E is the pion trajectory. Another test for the pion trajectory can be made by examining the density matrix elements ρ_{33}, $\mathrm{Re}\rho_{31}$, $\mathrm{Re}\rho_{3-1}$ for the Δ^{++} decay. The values which we obtained for the density matrix elements, using the method of moments, are listed in Table III, along with the predictions for OPE with absorption. The results are consistent with pion exchange at the p-Δ^{++} vertex. In our analysis we assume only that M is the Pomeron and try to obtain information on the exchange trajectory E. With this in mind, we write the triple-Regge invariant cross section as follows:

$$f(s,t,M_X^2/s) = \beta(t)(M_X^2/s)^{\alpha_P(0)-2\alpha_E(t)} s^{\alpha_P(0)-1}, \tag{14}$$

where $\beta(t)$ is a residue function, $\alpha_P(0) = 1.0$ is the intercept of the Pomeron trajectory, $\alpha_E(t)$ is the trajectory of the exchanged particle E, and M_X is the mass recoiling off the Δ^{++}, or the total energy of the aE system.

In order to determine the trajectory α_E, one generally fits expression (14) to the M_X^2/s distribution for various t intervals in the region where the model is valid. In this case, due to the width of the Δ^{++} resonance, the maximum value of M_X^2 kinematically allowed depends on the mass of the particular $p\pi^+$ considered. To remove this problem, we define the quantity[13] $z = M_X^2/M_{\max}^2$, where $M_{\max}^2$ is the maximum possible value of M_X^2 for any given t and $p\pi^+$ mass value. This distribution was obtained for each reaction for all events with $1.12 < M(p\pi^+) < 1.32$ GeV (which, as we have shown earlier, give a good representation of the Δ^{++} resonance behavior) for several regions of t. We fitted each z distribution by the form $z^{b(t)}$, where $b(t) = \alpha_P(0) - 2\alpha_E(t) \simeq 1 - 2\alpha_E(t)$. The data points shown in Fig. 8 are the results of these fits. The solid line in each case is the expected π trajectory, $\alpha_\pi(t) = 0.02 + t$, and the dotted lines are the ρ trajectory $\alpha_\rho(t) = 0.56 + t$. All four reactions are consistent with the exchange E being a π trajectory. Similar studies at lower energies for π^-p (Ref. 5) and K^-p (Ref. 16) interactions found that α_E is consistent with a π trajectory at low t [$\lesssim$0.3

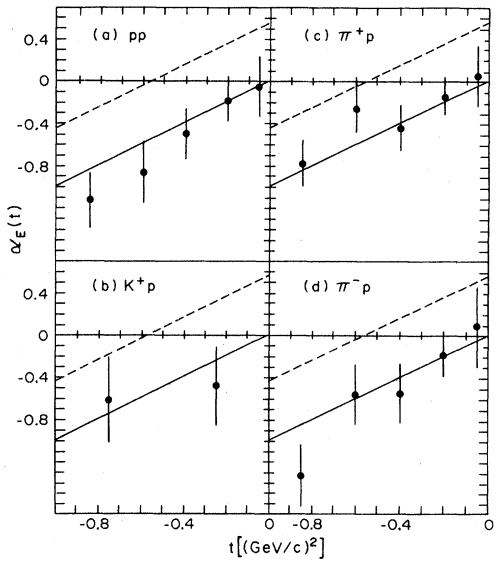

FIG. 8. Regge-trajectory parameters $\alpha_E(t)$ as a function of t as determined by the present analysis (see text) for (a) pp, (b) K^+p, (c) π^+p, and (d) π^-p interactions. The solid lines correspond to the pion trajectory and are of the form $\alpha_\pi = 0.02$ (GeV/c)$^2 + t$, and the dotted lines are the ρ trajectory $\alpha_\rho = 0.56$ (GeV/c)$^2 + t$.

$(\mathrm{GeV}/c)^2$] and with a ρ trajectory at higher t. Our results indicate that the contribution from ρ exchange has diminished with increasing energy and that at our energy, the one-pion-exchange diagram is dominant.

VI. SUMMARY

We have measured the inclusive Δ^{++} production at 147 GeV/c in pp, K^+p, π^+p, and π^-p interactions. All four reactions were measured with the same apparatus and analyzed in the same way.

We have studied the energy dependence of the Δ^{++} production for all four reactions by evaluating the Δ^{++} cross section in our experiment and from published data at other energies in a way consistent within each reaction. We found that the Δ^{++} cross section is consistent with $Ap^{-1}+B$ for the first three reactions in which the recoiling system off the Δ^{++} is neutral and may contain resonances. Similar energy dependence has been seen in another reaction [$\bar{p}p \to \Delta^{++}X^{--}$(Ref. 7)], where the system recoiling off the Δ^{++} could also contain resonances. Reaction (4) is constant with energy, as expected for a system in which the recoiling mesonic mass is doubly negatively charged. The same trend was found also for the reaction $K^-p \to \Delta^{++}X^{--}$.[13] These results indicate that in all four reactions only Pomeron exchange remains at the beam vertex at our energy.

We have also measured the Δ^{++} cross section for all four reactions at 147 GeV/c using the same Breit-Wigner shape and the same expression for the background. This permitted a study of the dependence of the Δ^{++} production on the beam properties. The inclusive distributions of the variables x, y, t', and p_T^2 all have very similar shapes for the different reactions, and their magnitudes, as well as those of the integrated cross sections, are proportional to their total cross sections. This result is expected if the dominant exchange at the beam vertex of the diagram in Fig. 7 is a Pomeron and if, in addition, all four reactions have the same exchange at the $p\Delta^{++}$ vertex.

We have studied the decay density matrix elements for the Δ^{++} decay, which gave results in good agreement with that of a Reggeized π-exchange model with absorption.[15]

We have studied the Δ^{++} recoil system using a triple-Regge analysis. We have obtained the effective trajectory of the exchange at the $p\Delta^{++}$ vertex and found for all four reactions that it is in good agreement with a pion trajectory.

ACKNOWLEDGMENTS

This work was supported in part by the U.S. Department of Energy, the National Science Foundation, the U.S.-Israel Binational Science Foundation, and the Dutch F.O.M. We gratefully acknowledge the efforts of the 30-inch bubble-chamber crew and the scanning and measuring personnel at the participating institutions.

---

*Present address: Eastern Illinois University, Charleston, Illinois.
†Present address: Dialog Systems, Belmont, Massachusetts.
‡Present address: Universite de Neuchatel, Neuchatel, Switzerland.
§Present address: Stanford Linear Accelerator Center, Stanford, California.
‖On leave of absence from The Weizmann Institute of Science, Rehovot, Israel.
¶On leave of absence from Tel-Aviv University, Ramat-Aviv, Israel.
**On leave of absence from College de France, Paris, France.
††Present address: Tufts University, Medford, Massachusetts.
‡‡Present address: Rockefeller University, New York, New York.
§§Present address: Fermi National Accelerator Laboratory, Batavia, Illinois.
‖‖Present address: Brookhaven National Laboratory, Upton, New York.

[1]D. Brick *et al.*, Phys. Rev. D 18, 3099 (1978).
[2]D. Fong *et al.*, Phys. Lett. B53, 290 (1974); *ibid.* B60, 124 (1975); Nucl. Phys. B102, 386 (1976); Phys. Lett. B61, 99 (1976); Nucl. Phys. B104, 32 (1976); Nuovo Cimento 34A, 659 (1976); Phys. Rev. Lett. 37, 736 (1976); F. Barreiro *et al.*, Nucl. Phys. B148, 41 (1979); D. Brick *et al.*, Phys. Rev. D 19, 743 (1979); Nucl. Phys. B150, 109 (1979); D. Brick *et al.*, work presented at the XIX International Conference on High Energy Physics, Tokyo, Japan, 1978 (unpublished).
[3]J. Bartke *et al.*, Nucl. Phys. B137, 189 (1978).
[4]S. J. Barish *et al.*, Phys. Rev. D 12, 1260 (1975).
[5]F. Barreiro *et al.*, Phys. Rev. D 17, 681 (1978).
[6]P. D. Higgins *et al.*, Phys. Rev. D 19, 731 (1979).
[7]D. R. Ward *et al.*, Nucl. Phys. B141, 203 (1978).
[8]E. G. Boos *et al.*, Nucl. Phys. B151, 193 (1979).
[9]P. Granet *et al.*, Nucl. Phys. B140, 389 (1978).
[10]J. D. Jackson, Nuovo Cimento 34, 1644 (1965).
[11]J. V. Beaupre *et al.*, Nucl. Phys. B67, 413 (1973).
[12]S. Ratti, private communication. The point for 11 GeV/c is calculated from data presented in P. Borzatta *et al.*, Nuovo Cimento 15A, 45 (1973).
[13]P. V. Chliapnikov, in *High Energy Physics*, Proceedings of the European Physical Society International Conference, Palermo, 1975, edited by A. Zichichi (Editrice Compositori, Bologna, 1976), p. 897.
[14]H. M. Chan *et al.*, Phys. Rev. Lett. 26, 672 (1971).
[15]E. Gotsman, Phys. Rev. D 9, 1575 (1974).
[16]A. C. Borg *et al.*, Nuovo Cimento 34A, 21 (1976).